Design and Implementation of a Portable Laser Calibration System for LHAASO-WFCTA

Guotao Yuan,[a,*] **Qinning Sun,**[a] **Min Jin,**[a] **Junji Xia,**[a] **Jing Liu,**[a] **Zhen Min,**[b,c] **Fengrong Zhu,**[a] **Long Chen,**[a,*] **Yang Wang,**[a] **Yu Liu**[a] **and Yong Zhang**[b] **on behalf of the LHAASO Collaboration**

[a]*School of Physical Science and Technology, Southwest Jiaotong University, Chengdu, 611756, Sichuan Province, China*

[b]*Key Laboratory of Particle Astrophyics Experimental Physics Division Computing Center, Institute of High Energy Physics, Chinese Academy of Sciences, 100049 Beijing, China*

[c]*TIANFU Cosmic Ray Research Center, Institute of HighEnergy Physics, Chinese Academy of Sciences Chengdu, 610000, Sichuan Province, China*

E-mail: longchen@swjtu.edu.cn

The Wide Field of View Cherenkov Telescope Array (WFCTA), situated in the harsh environment of Daocheng, is established to investigate ultrahigh energy cosmic rays. To enhance the calibration of WFCTA, a portable laser calibration system has been developed, which provides specified energy and direction of the YAG laser. Special designs, including power system, north calibration, and rotating system, have been implemented to ensure the proper functioning of the portable laser calibration system. The aluminum alloy of the entire frame and the vibration damper provide robust anti-impact ability and safety during transportation to different observation locations. A temperature control facility has been employed to meet the operational temperature requirement of electronic equipment. Various sensors have been utilized to monitor environmental parameters, the energy of YAG laser pulses, azimuth and pitch angles, and other parameters in real-time. The auto-control program is communicated wirelessly to avoid any manual interference with the system. The field experiment results have confirmed the reliability of the system and its ability to meet the calibration requirements of WFCTA.

---

*Speaker

PoS(ICRC2023)498

1. Introduction

As one of the major national science and technology infrastructures, the Large High Altitude Air Shower Observatory(LHAASO) located in Daocheng Haizi Mountain National Nature Reserve with an altitude of 4410 m [1, 2], consists of 3 major interconnected parts, Kilometer Square array(KM2A), Water Cherenkov Detector Array(WCDA), and the Wide Field of view Cherenkov Telescope Array(WFCTA). The aim of the WFCTA including 18 telescopes, is to measure the spectrum of cosmic rays from 10 TeV to 1 EeV by counting the number of photons detected [3, 4]. Thus, the calibration for WFCTA is crucial to the accuracy of the energy of the measured cosmic ray [5]. However, the distribution of the aerosol in the field of the telescope will give a challenge for the measurement by scattering the Cherenkov light with complicated function [6]. In the field of laser calibration, an end-to-end approach is adopted in Auger to measure the aerosol attenuation [7, 8]. Telescope located in four sites operated at clear nights, measure the molecular and aerosol scattering in the near UV by the Central Laser Facility(CLF) and the eXtreme Laser Facility (XLF) [9]. WFCTA also employed 3 nitrogen laser calibration systems (L2, L4, L5 shown in Figure 1) and 1 YAG laser calibration system about 1.5 km away from WFCTA (L3 shown in Figure 1) to measure the distribution of aerosol near the array of telescopes [10–12]. To better understand the aerosol or avoid the influence of the aerosol for the calibration, a portable laser calibration system with 355 nm is developed shown in 1. The system could be operated in the harsh environment outside of the LHAASO, where have a long distance away from WFCTA to ensure the laser beam track in the view of WFCTA is high enough that there is almost no aerosol scattering. This can simplify the laser calibration for the WFCTA.

In this paper, the main characters of the portable laser system is described. In Sec.2 the design of the total system, as well as the damping system and horizontal control system will be introduced. In Sec.3 operation of the portable laser calibration system will be presented.

2. Hardware description

The heart of the system is a YAG laser, which produces a linearly polarized beam of 355 nm light. The beam is pulsed with the maximum energy of about 2 mJ. To protect the laser, the portable laser calibration system is composed of aluminum alloy. Due to different implementation objectives, the system divided into three cavity for separate control as shown in Figure 2. The left compartment is the control cavity. The laser's water tank is fixed to the aluminum alloy using acrylic plates. The 24V DC power supply for sensor power and the Moxa for signal transmission are secured to the aluminum alloy slot using boat-shaped nuts. This compartment is used for placing various controllers and does not have high temperature and stability requirements. Due to the presence of insulation panels and the majority of heat producers within the system, the generated temperature during operation can maintain the normal functioning of the equipment within the compartment.

To avoid temperature interference with the optical cavity, insulation material is used to create a partition in the middle. The right compartment is the optical system, which houses an optical platform in the middle, and secure the laser and a beam path consisting of two mirrors and a BS spectroscope on the optical platform.One beam of light transmitted horizontally is collected by the energy probe as a reference beam, while the other beam directed vertically upwards is sent into the
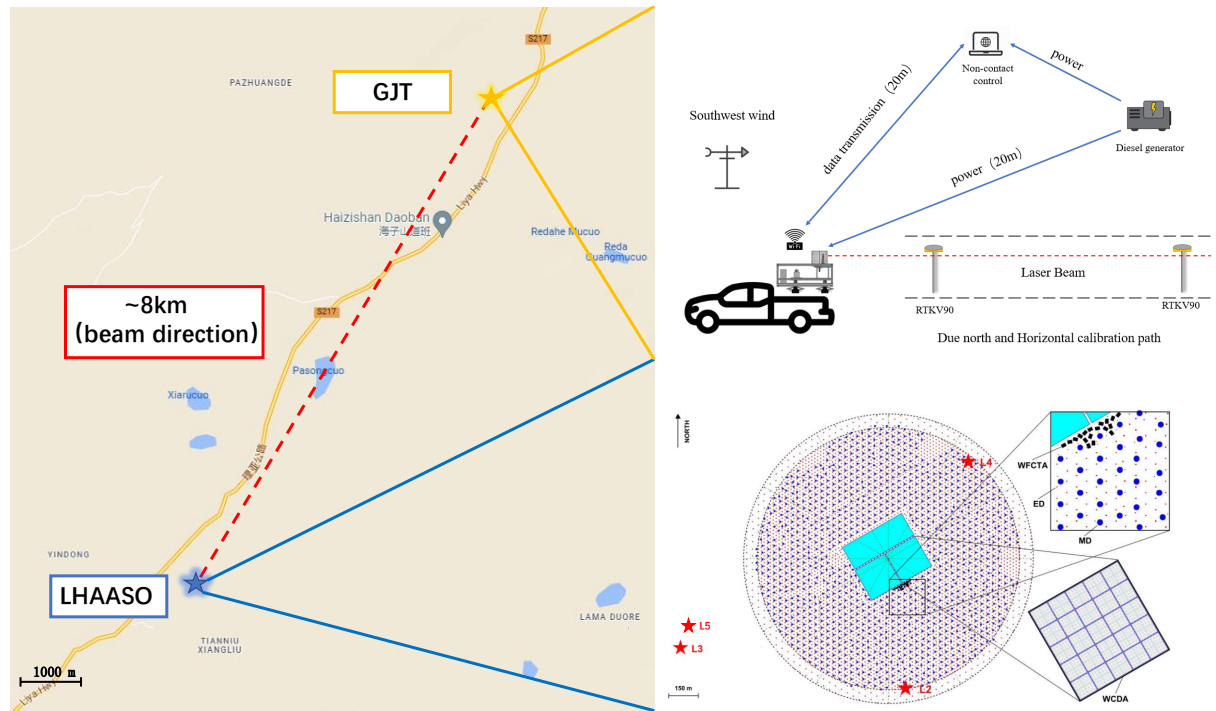
Figure 1: The layout of the LHAASO and GJT experimental sites is shown. The two locations are 8 km apart. The lower right image displays the layout of the LHAASO site and the L2 L5 lidar stations within the WFCTA. The upper right image illustrates the experimental setup of the portable laser calibration system at GJT.

rotation cavity as a calibration beam [12], another energy probe is located in the rotation cavity and measures the energy of the calibration beam before observation. The optical system is equipped with a temperature control and a damping system to ensure the stable operation of the laser and maintain the quality of the emitted laser beam. The rotating system is located above the optical system and consists of two URS100BPP units and an acrylic protective cover. The URS100BPP units are responsible for controlling the pitch and azimuth angles of the optical path. The calibration beam enters from the bottom and, after passing through the reflective mirror, is emitted from the emission slot, directed towards the telescope. The protective cover effectively shields the rotating cavity from external factors such as temperature variations and strong winds, ensuring the stability of the optical path in outdoor environments. The layout of the laser and instruments is shown in Figure 3(b).

Besides, a Real-Time Kinematic (RTK) system for positioning purposes, combined with the direction control system, is utilized to adjust the laser emission to the due north and horizontal directions. The system is powered by a portable power supply through a voltage regulator, ensuring stable operation. To prevent objective factors from affecting aerosol measurements, a auto-control system that matches the calibration system has been designed. The timing system provides a pulse trigger signal for the YAG laser, recording the time of each laser beam. This system can ensure the stable operation of laser cruising missions at night and support the implementation of over 80 different emission angles.
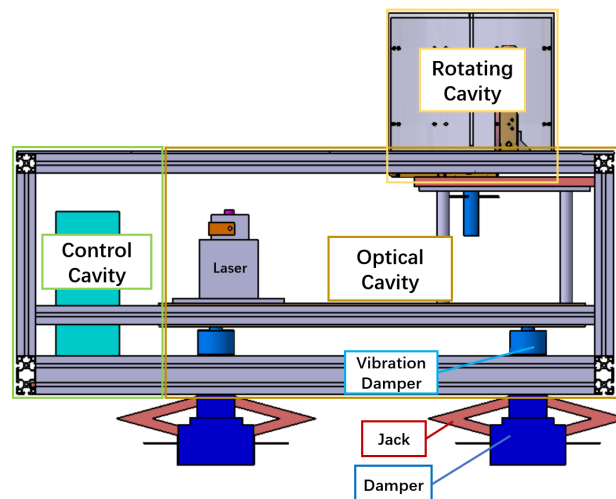
Figure 2: The schematic of the portable laser calibration system, divided into three cavities, control cavity in the green border, optical cavity in the brown border, rotating cavity in the orange border. The YAG laser placed in the optical table, supported by jack and damper below.

(a)	(b)

Figure 3: (a): The aluminum alloy framework of the laser calibration system, indicated by the blue portion, is insulated with insulating material, the insulation layer used to divide the cavities in the figure is temporarily removed. Acrylic panels are fixed on the outer side of the frame as a protective layer; (b): The schematic of the laser calibration system.

2.1 Framework

The framework of the portable laser calibration system is crucial for placing and protecting various sensors: Nd:YAG laser, optical platform, energy probe, etc. Cause of aluminum framework has the characteristics of processability and strong load-bearing capacity, the framework consists of different sizes of aluminum alloy, including 4040(height 40 mm × width 40 mm), 4080, 8080 shown as Figure 3(a), the connection points between them are secured using bolts. In the horizontal direction, M8 threaded holes are tapped from the middle of the aluminum alloy and bolts are used for fixation. In the vertical direction, M6 bolts are used for fastening. This designed framework can load more than 1000 kg, which ensures the sufficient firm of the system. There is a 2 mm-wide gap in the middle of each aluminum framework to accommodate the acrylic plate and insulation material. The gap is also utilized for securing components, bolts with a boat-shaped structure are

used in the fastening method.

2.2 Damping system

The damping system can help reduce the impact on the system and optical path, so it is divided into two parts: portable shock absorption and working shock absorption. portable shock absorption is mainly used to mitigate impacts caused during transportation. Carbon steel BK spring type damper are employed as the primary approach for transportation, as depicted in Figure 2. Four BK-080-S spring dampers are symmetrically installed below the framework, with an M10 bolt on each damper. Therefore, an adapter is designed to fasten the damper to the aluminum framework. The adapter and damper are both designed to be 150 mm in height. This height ensures that the dampers are fully loaded when the jack is retracted during operation. It also guarantees that during system operation, when the jack is lowered, the dampers are completely suspended without affecting the horizontal adjustment of the optical platform. On-site laser emitting in the wild, the optical path may be affected by slight vibrations due to various external forces. The working shock absorption is employed to reduce vertical vibrations of the optical platform, witch includes four LIVA-050-VD air cushion dampers installed below the optical platform. Additionally, eight rubber shock pads are afffixed to all four sides of the optical platform to reduce the horizontal vibrations. The damping system significantly reduces the impact of shock or vibration from the earth or the car on the optical path during the observation process. The URS100BPP units control the direction of the emitted laser beam. However, the horizontality of the optical platform in the optical system can influence the laser emitted point of the reflector in the rotating system. The horizontal adjustment of the optical platform is achieved by symmetrically adjusting the four jacks installed at the bottom of the aluminum framework. These jacks provided a height adjustment range of 124 mm to 420 mm, with a maximum adjustable angle of 26.7°. This ensures that the portable laser calibration system can be adjusted to maintain horizontal alignment during experiments at different wild locations. During adjustment, the inclinometer fixed on the optical platform measures the inclination of the current optical platform. And it would be recorded through numerical values on different axes, and monitored all the night as an indicator of operational stability, which illustrated in Figure 4.

2.3 Auto-control system

During system operation, the vibrations caused by close-range operations have a significant impact on the pointing accuracy of the laser. Additionally, to facilitate timed observations at multiple angles in a cyclic manner. A auto-control system specifically designed for portable laser calibration systems is designed shown as Figure 5. The system includes the display and recording of temperature, humidity, angle, laser energy, voltage, current and other information, as well as the control of rotary displacement table, calibration of the due north and horizontal, multi angle automatic cruise and other functions. There is a distance of 50 m between the equipment and the system, after the location fixed, auto-control can be achieved.

2.4 Power supply

The laser experimental site is typically located in remote areas, often in high-altitude mountainous regions, where there is no access to a fixed power supply. Power is provided by a portable fuel
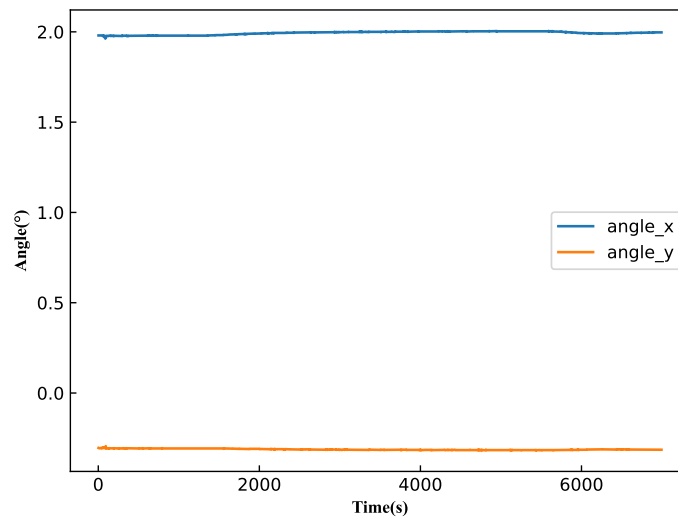
Figure 4: The framework of the inclined angle recorded every three seconds throughout the night on October 26th, 2022. The angle fluctuation remained around 5% throughout the night.
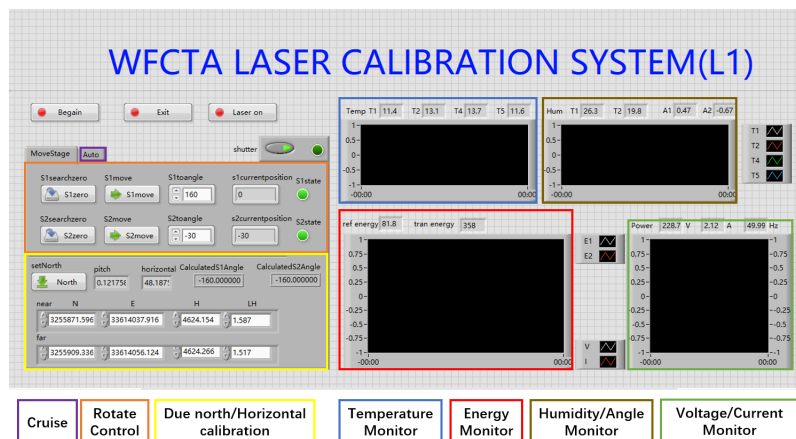
Figure 5: auto-control system, which provided adjustments for the north and horizontal alignment, and the environmental and energy monitoring, and rotational control.

generator with a maximum power output of 10 kW. To ensure a stable voltage supply, a 5 kW voltage regulator is placed between the generator and the system. The system itself has a maximum power consumption of 2 kW. Considering the challenging operating conditions in high-altitude areas, a redundancy of 3 kW is reserved to account for any potential impacts on the equipment's performance. ESP301 controller, laser, and other precision instruments will burn out electrical appliances when the voltage is unstable. Connect a voltage stabilizing source between the Diesel generator and electrical equipment to stabilize the voltage. One power supply is supplied to the control computer and the other to the calibration system. The energy probe, WIFI, 24 V DC power supply module, thyristor, temperature controller, shutter, and rotary displacement table in the calibration system

are powered by 220V plug-in. The temperature and humidity sensor, hub, current sensor, voltage sensor, 3.3 V power supply module, and MOXA are powered by 24 V DC power supply module, while the LED driver board and GPS are powered by 3.3 V power supply module. The signal wires of sensors, energy probes, and other devices are connected in parallel to MOXA, which connects to WIFI. Data and instructions interact between the device and the control computer through a local area network.

3. Operation

In a clear night, the portable laser calibration system is transported to the experimental site. After fixing the device, activating the portable power source and emitting the laser pulse with an external trigger TTL for preheating, the remote contact control system is activated to adjust the jack and the position of the optical platform based on the angle information provided by the inclinometer. A flat direction is chosen as the measurement path, and the laser beam is rotated in that direction while simultaneously recording the position information. In collaboration with RTKV90, the elevation, due north, and east coordinates of two points are determined. The deviation between the current direction and due north, as well as the horizontal direction is calculate and corrected. The adjusted values for true north and horizontal position are set as the initial emission values, and the laser direction is adjusted to shoot into the energy probe for a measurement period of half an hour. Once the measurement is completed, the system transitions to the cruise phase according to the predetermined cruise plan.

4. Summary

Many accessories are designed to ensure the accuracy of the emitted angle and the pulse energy of the laser for the calibration of WFCTA. Completing this system in as small space as possible gives a great challenge. By designing a multi-cavities structure and arranging different subsystems according to their specific requirements, the system is successfully completed. Furthermore, the experimental data at GJT with L1 will be analyzed to give more information about the calibration.

References

[1] Zhen C, Ming-Jun C, Song-Zhan C, et al. Introduction to large high altitude air shower observatory (LHAASO)[J]. Chinese Astronomy and Astrophysics, 2019, 43(4): 457-478.

[2] Feng Z, Hu L, Feng-Rong Z. Properties of secondary components in extensive air shower of cosmic rays in knee energy region[J]. ACTA PHYSICA SINICA, 2022, 71(24).

[3] He H, LHAASO collaboration. Design of the LHAASO detectors[J]. Radiation Detection Technology and Methods, 2018, 2: 1-8.

[4] Zhang S S, Bai Y X, Cao Z, et al. Properties and performance of two wide field of view Cherenkov/fluorescence telescope array prototypes[J]. Nuclear Instruments and Methods in Physics Research Section A: Accelerators, Spectrometers, Detectors and Associated Equipment, 2011, 629(1): 57-65.

[5] Aharonian F, An Q, Bai L X, et al. Absolute calibration of LHAASO WFCTA camera based on LED[J]. Nuclear Instruments and Methods in Physics Research Section A: Accelerators, Spectrometers, Detectors and Associated Equipment, 2022, 1021: 165824.

[6] Li X, Chen Q H, Liu H, et al. Study on the Variability of Extinction Coefficients of Atmospheric Aerosol Over LHAASO[J]. 2019.

[7] Mussa R, Argiro S, Cester R, et al. The LIDAR systems for atmospheric monitoring in Auger[J]. Nuclear Instruments and Methods in Physics Research Section A: Accelerators, Spectrometers, Detectors and Associated Equipment, 2004, 518(1-2): 183-185.

[8] Fick B, Malek M, Matthews J A J, et al. The central laser facility at the Pierre Auger Observatory[J]. Journal of Instrumentation, 2006, 1(11): P11003.

[9] Pierre Auger Collaboration. Techniques for measuring aerosol attenuation using the Central Laser Facility at the Pierre Auger Observatory[J]. Journal of Instrumentation, 2013, 8(04): P04009.

[10] Chen L, Li X, Ge L, et al. Application of the nitrogen laser calibration system in LHAASO-WFCTA[J]. 2021.

[11] Wang Y, Chen L, Liu H, et al. The Laser calibration system for LHAASO-WFCTA[J]. 2022.

[12] Sun Q N, Geng L S, Li X, et al. The YAG Lidar System Applied in LHAASO[J]. 2021.

[13] Sun Q, Xie L, Yuan G, et al. Design and development of laser temperature control system of LHAASO[J]. Journal of Instrumentation, 2023, 18(06): T06008.

Full Authors List: Collaboration

Zhen Cao[1,2,3], F. Aharonian[4,5], Q. An[6,7], Axikegu[8], L.X. Bai[9], Y.X. Bai[1,3], L.X. Bai[9], Y.X. Bai[1,3], Y.W. Bao[10], D. Bastieri[11], X.J. Bi[1,2,3], Y.J. Bi[1,3], H. Cai[12], J.T. Cai[11], Zhe Cao[6,7], J. Chang[13], J.F. Chang[1,3,6], B.M. Chen[14], E.S. Chen[1,2,3], J. Chen[9], Liang Chen[1,2,3], Liang Chen[15], Long Chen[8], M.J. Chen[1,3], M.L. Chen[1,3,6], Q.H. Chen[8], S.H. Chen[1,2,3], S.Z. Chen[1,3], T.L. Chen[16],X.L. Chen[1,2,3], Y. Chen[10], N. Cheng[1,3], Y.D. Cheng[1,3], S.W. Cui[14], X.H. Cui[17], Y.D. Cui[18], B. D'Ettorre Piazzoli[19], B.Z. Dai[20], H.L. Dai[1,3,6], Z.G. Dai[7], Danzengluobu[16], D. della Volpe[21], X.J. Dong[1,3], K.K. Duan[13], J.H. Fan[11], Y.Z. Fan[13], Z.X. Fan[1,3], J. Fang[20], K. Fang[1,3], C.F. Feng[22], L. Feng[13], S.H. Feng[1,3], Y.L. Feng[13], B. Gao[1,3], C.D. Gao[22], L.Q. Gao[1,2,3], Q. Gao[16], W. Gao[22], M.M. Ge[20], L.S. Geng[1,3], G.H. Gong[23], Q.B. Gou[1,3], M.H. Gu[1,3,6], F.L. Guo[15], J.G. Guo[1,2,3], X.L. Guo[8], Y.Q. Guo[1,3], Y.Y. Guo[1,2,3,13], Y.A. Han[24], H.H. He[1,2,3], H.N. He[13], J.C. He[1,2,3], S.L. He[11], X.B. He[18], Y. He[8], M. Heller[21], Y.K. Hor[18], C. Hou[1,3], H.B. Hu[1,2,3], S. Hu[9], S.C. Hu[1,2,3], X.J. Hu[23], D.H. Huang[8], Q.L. Huang[1,3], W.H. Huang[22], X.T. Huang[22], X.Y. Huang[13], Z.C. Huang[8], F. Ji[1,3], X.L. Ji[1,3,6], H.Y. Jia[8], K. Jiang[6,7], Z.J. Jiang[20], C. Jin[1,2,3], T. Ke[1,3], D. Kuleshov[25], K. Levochkin[25], B.B. Li[14], Cheng Li[6,7], Cong Li[1,3], F. Li[1,3,6], H.B. Li[1,3], H.C. Li[1,3], H.Y. Li[7,13], J. Li[1,3,6], K. Li[1,3], W.L. Li[22], X.R. Li[1,3], Xin Li[6,7], Xin Li[8], Y. Li[9], Y.Z. Li[1,2,3], Zhe Li[1,3], Zhuo Li[26], E.W. Liang[27], Y.F. Liang[27], S.J. Lin[18], B. Liu[7], C. Liu[1,3], D. Liu[22], H. Liu[8], H.D. Liu[24], J. Liu[1,3], J.L. Liu[28], J.S. Liu[18], J.Y. Liu[1,3], M.Y. Liu[16], R.Y. Liu[10], S.M. Liu[8], W. Liu[1,3], Y. Liu[11], Y.N. Liu[23], Z.X. Liu[9], W.J. Long[8], R. Lu[20], H.K. Lv[1,3], B.Q. Ma[26], L.L. Ma[1,3], X.H. Ma[1,3], J.R. Mao[29], A. Masood[8], Z. Min[1,3], W. Mitthumsiri[30], T. Montaruli[21], Y.C. Nan[22], B.Y. Pang[8], P. Pattarakijwanich[30], Z.Y. Pei[11], M.Y. Qi[1,3], Y.Q. Qi[14], B.Q. Qiao[1,3], J.J. Qin[7], D. Ruffolo[30], V. Rulev[25], A. Sáiz[30], L. Shao[14], O. Shchegolev[25,31], X.D. Sheng[1,3], J.Y. Shi[1,3], H.C. Song[26], Yu.V. Stenkin[25,31], V. Stepanov[25], Y. Su[32], Q.N. Sun[8], X.N. Sun[27], Z.B. Sun[33], P.H.T. Tam[18], Z.B. Tang[6,7], W.W. Tian[2,17], B.D. Wang[1,3], C. Wang[33], H. Wang[8], H.G. Wang[11], J.C. Wang[29], J.S. Wang[28], L.P. Wang[22], L.Y. Wang[1,3], R.N. Wang[8], W. Wang[18], W. Wang[12], X.G. Wang[27], X.J. Wang[1,3], X.Y. Wang[10], Y. Wang[8], Y.D. Wang[1,3], Y.J. Wang[1,3], Y.P. Wang[1,2,3], Z.H. Wang[9], Z.X. Wang[20], Zhen Wang[28], Zheng Wang[1,3,6], D.M. Wei[13], J.J. Wei[13], Y.J. Wei[1,2,3], T. Wen[20], C.Y. Wu[1,3], H.R. Wu[1,3], S. Wu[1,3], W.X. Wu[8], X.F. Wu[13], S.Q. Xi[1,3], J. Xia[7,13], J.J. Xia[8], G.M. Xiang[2,15], D.X. Xiao[16], G. Xiao[1,3], H.B. Xiao[11], G.G. Xin[12], Y.L. Xin[8], Y. Xing[15], D.L. Xu[28], R.X. Xu[26], L. Xue[22], D.H. Yan[29], J.Z. Yan[13], C.W. Yang[9], F.F. Yang[1,3,6], J.Y. Yang[18], L.L. Yang[18], M.J. Yang[1,3], R.Z. Yang[7], S.B. Yang[20], Y.H. Yao[9], Z.G. Yao[1,3], Y.M. Ye[23], L.Q. Yin[1,3], N. Yin[22], X.H. You[1,3], Z.Y. You[1,2,3], Y.H. Yu[22], Q. Yuan[13], H.D. Zeng[13], T.X. Zeng[1,3,6], W. Zeng[20], Z.K. Zeng[1,2,3], M. Zha[1,3], X.X. Zhai[1,3], B.B. Zhang[10], H.M. Zhang[10], H.Y. Zhang[22], J.L. Zhang[17], J.W. Zhang[9], L.X. Zhang[11], Li Zhang[20], Lu Zhang[14], P.F. Zhang[20], P.P. Zhang[14], R. Zhang[7,13], S.R. Zhang[14], S.S. Zhang[1,3], X. Zhang[10], X.P. Zhang[1,3], Y.F. Zhang[8], Y.L. Zhang[1,3], Yi Zhang[1,13], Yong Zhang[1,3], B. Zhao[8], J. Zhao[1,3], L. Zhao[6,7], L.Z. Zhao[14], S.P. Zhao[13,22], F. Zheng[33], Y. Zheng[8], B. Zhou[1,3], H. Zhou[28], J.N. Zhou[15], P. Zhou[10], R. Zhou[9], X.X. Zhou[8], C.G. Zhu[22], F.R. Zhu[8], H. Zhu[17], K.J. Zhu[1,2,3,6] and X. Zuo[1,3]

[1]Key Laboratory of Particle Astrophyics & Experimental Physics Division & Computing Center, Institute of High Energy Physics, Chinese Academy of Sciences, 100049 Beijing, China.
[2]University of Chinese Academy of Sciences, 100049 Beijing, China.
[3]TIANFU Cosmic Ray Research Center, Chengdu, Sichuan, China.
[4]Dublin Institute for Advanced Studies, 31 Fitzwilliam Place, 2 Dublin, Ireland.
[5]Max-Planck-Institut for Nuclear Physics, P.O. Box 103980, 69029 Heidelberg, Germany.
[6]State Key Laboratory of Particle Detection and Electronics, China.
[7]University of Science and Technology of China, 230026 Hefei, Anhui, China.
[8]School of Physical Science and Technology & School of Information Science and Technology, Southwest Jiaotong University, 610031 Chengdu, Sichuan, China.
[9]College of Physics, Sichuan University, 610065 Chengdu, Sichuan, China.
[10]School of Astronomy and Space Science, Nanjing University, 210023 Nanjing, Jiangsu, China.
[11]Center for Astrophysics, Guangzhou University, 510006 Guangzhou, Guangdong, China.
[12]School of Physics and Technology, Wuhan University, 430072 Wuhan, Hubei, China.
[13]Key Laboratory of Dark Matter and Space Astronomy, Purple Mountain Observatory, Chinese Academy of Sciences, 210023 Nanjing, Jiangsu, China.
[14]Hebei Normal University, 050024 Shijiazhuang, Hebei, China.
[15]Key Laboratory for Research in Galaxies and Cosmology, Shanghai Astronomical Observatory, Chinese Academy of Sciences, 200030 Shanghai, China.
[16]Key Laboratory of Cosmic Rays (Tibet University), Ministry of Education, 850000 Lhasa, Tibet, China.
[17]National Astronomical Observatories, Chinese Academy of Sciences, 100101 Beijing, China.
[18]School of Physics and Astronomy & School of Physics (Guangzhou), Sun Yat-sen University, 519000 Zhuhai, Guangdong, China.
[19]Dipartimento di Fisica dell'Università di Napoli `Federico II", Complesso Universitario di Monte Sant'Angelo, via Cinthia, 80126 Napoli, Italy.
[20]School of Physics and Astronomy, Yunnan University, 650091 Kunming, Yunnan, China.
[21]D'epartement de Physique Nucl'eaire et Corpusculaire, Facult'e de Sciences, Universit'e de Gen'eve, 24 Quai Ernest Ansermet, 1211 Geneva, Switzerland.
[22]Institute of Frontier and Interdisciplinary Science, Shandong University, 266237 Qingdao, Shandong, China.
[23]Department of Engineering Physics, Tsinghua University, 100084 Beijing, China.
[24]School of Physics and Microelectronics, Zhengzhou University, 450001 Zhengzhou, Henan, China.
[25]Institute for Nuclear Research of Russian Academy of Sciences, 117312 Moscow, Russia.

[26]School of Physics, Peking University, 100871 Beijing, China.

[27]School of Physical Science and Technology, Guangxi University, 530004 Nanning, Guangxi, China.

[28]Tsung-Dao Lee Institute & School of Physics and Astronomy, Shanghai Jiao Tong University, 200240 Shanghai, China.

[29]Yunnan Observatories, Chinese Academy of Sciences, 650216 Kunming, Yunnan, China.

[30]Department of Physics, Faculty of Science, Mahidol University, 10400 Bangkok, Thailand.

[31]Moscow Institute of Physics and Technology, 141700 Moscow, Russia.

[32]Key Laboratory of Radio Astronomy, Purple Mountain Observatory, Chinese Academy of Sciences, 210023 Nanjing, Jiangsu, China.

[33]National Space Science Center, Chinese Academy of Sciences, 100190 Beijing, China.